

Interlayer coupling effect on a bilayer Kitaev model

Hiroyuki Tomishige, Joji Nasu, and Akihisa Koga

Department of Physics, Tokyo Institute of Technology, Meguro, Tokyo 152-8551, Japan

(Received 25 December 2017; published 2 March 2018)

We investigate a bilayer Kitaev model in which two honeycomb layers are coupled by the Heisenberg interactions to discuss the effects of interlayer coupling on Kitaev quantum spin liquids (QSLs). In this model, there exists a local conserved quantity which results in no long-range spin correlations in the system. Using the exact diagonalization, bond-operator mean-field theory, and cluster expansion techniques, we study ground-state properties in the system. The obtained results suggest the existence of a first-order quantum phase transition between the Kitaev QSL and dimer-singlet states. We find that a one-triplet excitation from the dimer-singlet ground state is localized owing to the existence of the local conserved quantity. To examine finite-temperature properties, we make use of the thermal pure quantum state approach. We clarify that the double-peak structure in the specific heat inherent in the Kitaev QSL is maintained even above the quantum phase transition. The present results suggest that the Kitaev QSL is stable against the interlayer interference. Magnetic properties of multilayer Kitaev models are also addressed.

DOI: [10.1103/PhysRevB.97.094403](https://doi.org/10.1103/PhysRevB.97.094403)**I. INTRODUCTION**

Exploring quantum spin liquids (QSLs) has been one of the central subjects in condensed-matter physics since Anderson's suggestion [1–4]. Although a lot of theoretical and experimental studies have been devoted to clarifying the nature of QSLs, the thermodynamic properties and excitation spectra still remain elusive. Theoretically, it is still hard to reveal properties of frustrated Heisenberg models, which are regarded as archetypal models of QSLs, without approximations. On the other hand, one of the promising models to discuss QSLs is a quantum spin model on a honeycomb lattice with bond-dependent Ising interactions, which is known as the Kitaev model [5–7]. This model is exactly solvable, and its ground state is a QSL with short-range spin correlations [8,9]. Furthermore, quantum spins are fractionalized into itinerant Majorana fermions and localized Z_2 fluxes. This leads to gapless elementary excitations in the ground state and a double-peak structure in the specific heat [5,10–15]. Moreover, Jackeli and Khaliullin have suggested that the Kitaev model should be realizable in Mott insulators with strong spin-orbit coupling and specific lattice structure, where localized $j_{\text{eff}} = 1/2$ spins are coupled by the superexchange interactions [16]. As candidate materials, $A_2\text{IrO}_3$ ($A = \text{Na, Li}$) [17–20], $\alpha\text{-RuCl}_3$ [21–24], and $\text{H}_3\text{LiIr}_2\text{O}_6$ [25] have been proposed, and many experimental and theoretical studies have been done in terms of the Kitaev physics [9,14,15,26–46], including generalizations of the Kitaev model [47–49].

Nevertheless, it has been revealed that the magnetic properties at low temperatures in the candidate materials cannot be fully reproduced by the two-dimensional pure Kitaev model, while this model should capture the magnetism at higher temperatures. For instance, the materials exhibit a long-range magnetic order at low temperatures [17,18,21–24,50], and a star-shaped low-energy structure has been observed in inelastic neutron scattering experiments [28,29]. To account for these

features, additional effects beyond the pure Kitaev model, such as Heisenberg and/or Γ terms with or without long-range interactions [51–69] and intermediate spin-orbit coupling [70], have been theoretically studied recently. On the other hand, the candidate materials are composed of honeycomb layers, and the role of the stacking structure in $\alpha\text{-RuCl}_3$ and $\text{H}_3\text{LiIr}_2\text{O}_6$ has been examined recently [25,71,72]. While interlayer couplings in the stacked honeycomb compounds also exist, the previous theoretical studies mainly focused on the additional in-plane interactions. Therefore, it is highly desired to theoretically study the stability of the Kitaev QSL in the presence of interlayer coupling. Furthermore, controlling configurations of stacked layers in iridium and ruthenium compounds is becoming realistic [73–76], which stimulates further investigations into the effects of interlayer coupling.

In this paper, we study the bilayer Kitaev model, where two honeycomb layers are coupled by the Heisenberg interaction, which is introduced as one of the simplest couplings to extract the nature of the interlayer effect on the Kitaev QSL [see Fig. 1(a)]. We first show that this model possesses a local conserved quantity in each pair of stacked hexagons (bihexagon), which leads to the absence of the long-range magnetic order. To study the stability of the Kitaev QSL against interlayer coupling, we employ the bond-operator mean-field (MF) approximation [77] and the cluster expansion technique [78–80]. We also use the exact diagonalization (ED) on finite clusters to discuss ground-state properties and the excitation spectrum. The numerical results suggest the existence of a first-order phase transition between the Kitaev QSL and dimer-singlet states at zero temperature. Moreover, using the thermal pure quantum (TPQ) state approach [81,82], we clarify that the double-peak structure emerges in the small interlayer coupling region and is retained even above the quantum transition point expected from the ED calculations. We also extend the argument based on the presence of the local conserved quantities to a multilayer Kitaev model and show the absence

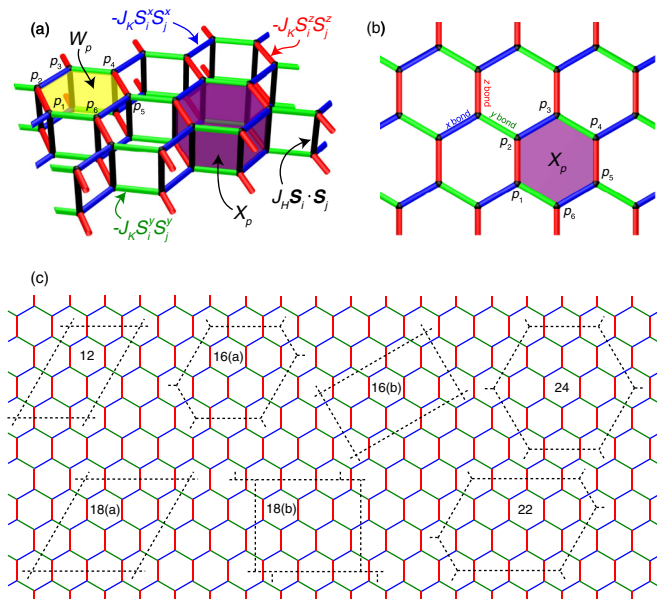


FIG. 1. (a) Bilayer Kitaev model on the honeycomb lattice. (b) Top view of the bilayer Kitaev model with the definition of dimer sites p_i for the local conserved quantity X_p . (c) Several clusters used in the ED calculations. The number shown in the plot represents the number of dimers N in the cluster, which includes $2N$ spins.

of three-dimensional long-range correlations in the multilayer Kitaev model with arbitrary stacking numbers.

This paper is organized as follows. In Sec. II, we introduce the model Hamiltonian on the bilayer honeycomb lattice and discuss the local conserved quantity and the parity symmetry in the system. Our methods are briefly summarized in Sec. III. In Sec. IV, we show the numerical results for the ground-state properties in the bilayer system, which suggests the existence of a first-order quantum phase transition between the QSL and dimer-singlet states. Thermodynamic properties are discussed in Sec. V. In Sec. VI, we discuss magnetic properties in the multilayer Kitaev model. A summary is provided in the last section.

II. THE MODEL AND ITS SYMMETRY

To address the effect of interlayer coupling between Kitaev models on honeycomb lattices, we introduce the following simple model, where two Kitaev models are coupled by the Heisenberg interaction [see Fig. 1(a)]:

$$\mathcal{H} = -J_K \sum_{\langle ij \rangle_{\alpha}, n} S_{i,n}^{\alpha} S_{j,n}^{\alpha} + J_H \sum_i \mathbf{S}_{i,1} \cdot \mathbf{S}_{i,2}, \quad (1)$$

where $S_{i,n}^{\alpha} = \frac{1}{2} \sigma_{i,n}^{\alpha}$ ($\alpha = x, y, z$) and $\sigma_{i,n}^{\alpha}$ is the Pauli matrix at site i of the n th ($=1, 2$) layer. J_K (>0) is the ferromagnetic Kitaev coupling in each layer, and J_H (>0) is the antiferromagnetic Heisenberg coupling between these two layers. We assume that each site on layer 1 is located just above that on layer 2. In each layer, the anisotropy of the Ising-type interactions depends on the bonds; there are three kinds of nearest-neighbor (NN) bonds $\langle ij \rangle_{\alpha}$ ($\alpha = x, y, z$), which we

refer to as the α bond, on the honeycomb lattice [see Figs. 1(a) and 1(b)].

When $J_H = 0$, the system is reduced to two monolayer Kitaev models. In the model, a local Z_2 conserved quantity $W_{p,n} = \sigma_{p_1,n}^x \sigma_{p_2,n}^y \sigma_{p_3,n}^z \sigma_{p_4,n}^x \sigma_{p_5,n}^y \sigma_{p_6,n}^z$ exists on the n th layer, which results in the QSL ground state with long-range spin entanglement and the fractionalization of the quantum spins. This allows us to map the monolayer model onto a free Majorana fermion system with gapless elementary excitations, although there exists a gap in the spin excitation. At finite temperatures, the spin fractionalization emerges as a peculiar temperature dependence of observables such as the double-peak structure in the specific heat [14, 15]. On the other hand, in the case of $J_K = 0$, the system is reduced to a system composed of independent dimers. The ground state is represented by the direct product of interlayer dimer singlets with the spin gap, where interdimer wave functions are disentangled. Although these two nonmagnetic ground states possess a spin gap, their low-energy properties are different from each other. Then, one naively expects a phase transition between these two states by changing the parameter $\lambda = J_H/J_K$.

The striking feature of this model is that a local conserved quantity exists. In the presence of interlayer coupling J_H , W_p no longer commutes with the Hamiltonian. Instead, the product $X_p = W_{p,1} W_{p,2}$ is a local Z_2 conserved quantity [see Fig. 1(b)]. This is because two spin operators with dimer site i in X_p on plaquette p have the same spin component, and X_p commutes with $\mathbf{S}_{i,1} \cdot \mathbf{S}_{i,2}$. As $X_p^2 = 1$, the eigenstates of the Hamiltonian given in Eq. (1) are characterized by the eigenvalue of X_p , ± 1 , in each bihexagon p . The existence of the local conserved quantity leads to the absence of spin correlations except for NN sites in each Kitaev layer and sites belonging to the same interlayer dimer. Thus, the ground state remains nonmagnetic even in the presence of interlayer coupling J_H .

To clarify another symmetry of the present bilayer Kitaev system given in Eq. (1), we adopt the bond-operator representation [77], which is useful for analyzing spin-dimer systems [83–85]. In this representation, the four local bases on each dimer i are described as

$$|s\rangle_i = s_i^{\dagger} |0\rangle = \frac{1}{\sqrt{2}} (|\uparrow\downarrow\rangle_i - |\downarrow\uparrow\rangle_i), \quad (2)$$

$$|t_x\rangle_i = t_{xi}^{\dagger} |0\rangle = -\frac{1}{\sqrt{2}} (|\uparrow\uparrow\rangle_i - |\downarrow\downarrow\rangle_i), \quad (3)$$

$$|t_y\rangle_i = t_{yi}^{\dagger} |0\rangle = \frac{i}{\sqrt{2}} (|\uparrow\uparrow\rangle_i + |\downarrow\downarrow\rangle_i), \quad (4)$$

$$|t_z\rangle_i = t_{zi}^{\dagger} |0\rangle = \frac{1}{\sqrt{2}} (|\uparrow\downarrow\rangle_i + |\downarrow\uparrow\rangle_i), \quad (5)$$

where s_i^{\dagger} and $t_{\alpha i}^{\dagger}$ ($\alpha = x, y, z$) are the creation operators of the singlet and triplets on dimer site i , respectively, and $|0\rangle$ is their vacuum. We assume that these bond operators behave as bosons and impose the local constraint $s_i^{\dagger} s_i + \sum_{\alpha} t_{\alpha i}^{\dagger} t_{\alpha i} = 1$ on each dimer i to reproduce the commutation relation of an $S = 1/2$ spin. By means of the bond operators, the Hamiltonian given

in Eq. (1) is rewritten as

$$\begin{aligned}
 \mathcal{H} = & -\frac{J_K}{2} \sum_{\langle ij \rangle_\alpha} \left(s_i s_j^\dagger t_{\alpha i}^\dagger t_{\alpha j} + s_i s_j t_{\alpha i}^\dagger t_{\alpha j}^\dagger + \text{H.c.} \right. \\
 & \left. - \sum_{\beta\beta'\gamma\gamma'} \epsilon_{\alpha\beta\gamma} \epsilon_{\alpha\beta'\gamma'} t_{\beta i}^\dagger t_{\beta' j}^\dagger t_{\gamma i}^\dagger t_{\gamma' j} \right) \\
 & + J_H \sum_i \left(-\frac{3}{4} s_i^\dagger s_i + \frac{1}{4} \sum_\alpha t_{\alpha i}^\dagger t_{\alpha i} \right) \\
 & - \sum_i \mu_i \left(s_i^\dagger s_i + \sum_\alpha t_{\alpha i}^\dagger t_{\alpha i} - 1 \right), \quad (6)
 \end{aligned}$$

where $\epsilon_{\alpha\beta\gamma}$ stands for the Levi-Civita symbol and μ_i is a Lagrange multiplier on each dimer to impose the local constraint.

We find that the number of each boson is not conserved, but bosons are created or annihilated as a pair in the boson sector of each kind. For example, the second line in Eq. (6) is expanded as $t_{iy}^\dagger t_{iz}^\dagger t_{jz}^\dagger t_{jy} - t_{iy}^\dagger t_{iz}^\dagger t_{jy}^\dagger t_{jz} + \text{H.c.}$ when $\alpha = x$. Therefore, the parity of the particle number is conserved for each component of the bosons. In other words, the parity operators $P_s = \exp[i\pi \sum_i s_i^\dagger s_i]$ and $P_{t_\alpha} = \exp[i\pi \sum_i t_{\alpha i}^\dagger t_{\alpha i}]$ ($\alpha = x, y, z$) commute with the Hamiltonian.

We note that the four local states on a dimer, $|s\rangle_i$, $|t_x\rangle_i$, $|t_y\rangle_i$, and $|t_z\rangle_i$, are the eigenstates of X_p since

$$\sigma_{i1}^\alpha \sigma_{i2}^\alpha |s\rangle_i = -|s\rangle_i, \quad \sigma_{i1}^\alpha \sigma_{i2}^\alpha |t_\beta\rangle_i = (1 - 2\delta_{\alpha\beta}) |t_\beta\rangle_i. \quad (7)$$

In addition, the number operators are given as projectors onto the singlet and triplet states:

$$s_i^\dagger s_i = \frac{1}{4} - \mathbf{S}_{i1} \cdot \mathbf{S}_{i2}, \quad t_{\alpha i}^\dagger t_{\alpha i} = \frac{1}{4} + \mathbf{S}_{i1} \cdot \mathbf{S}_{i2} - 2S_{i1}^\alpha S_{i2}^\alpha, \quad (8)$$

leading to the fact that each parity operator commutes with X_p . Therefore, eigenstates of the Hamiltonian are specified by the eigenvalues of $[P_{t_x}, P_{t_y}, P_{t_z}, \{X_p\}]$, each of which takes ± 1 . Note that P_s is determined by P_{t_α} due to the constraint $P_s = \prod_\alpha P_{t_\alpha}$. For example, for the state $|\Phi_s\rangle = \prod_i s_i^\dagger |0\rangle$, $P_{t_x} = P_{t_y} = P_{t_z} = +1$, and $X_p = +1$ for all plaquettes, which is schematically shown in Fig. 2(a). We also consider a state $|\Phi_{t_x}\rangle = t_{ix}^\dagger \prod_{j \neq i} s_j^\dagger |0\rangle = \tilde{t}_{ix}^\dagger |\Phi_s\rangle$, where the triplet excitation (triplon) creation operator from the singlet state is introduced as $\tilde{t}_{i\alpha}^\dagger = t_{i\alpha}^\dagger s_i$. This state is also an eigenstate of X_p with an eigenvalue of -1 for the two plaquettes sharing the x bond where the triplon is located on one of the edge sites [see Fig. 1(b)]. In this case, the eigenvalue of X_p is $+1$ for the other plaquettes p' . From the above discussion, one can determine the spatial configuration of eigenvalues of X_p , as shown in Fig. 2(b). The eigenvalues of X_p for the multiple-triplet excited state can also be discussed in the same manner, as shown in Fig. 2(c). Note that this is similar to the configuration of W_p for the state where a spin operator operates on the ground state in the monolayer Kitaev model. The details of the excitation spectrum of triplons are given in Sec. IV B.

III. METHODS

To analyze the properties of the ground state in Eq. (1), we mainly employ the ED method in finite-size clusters up to

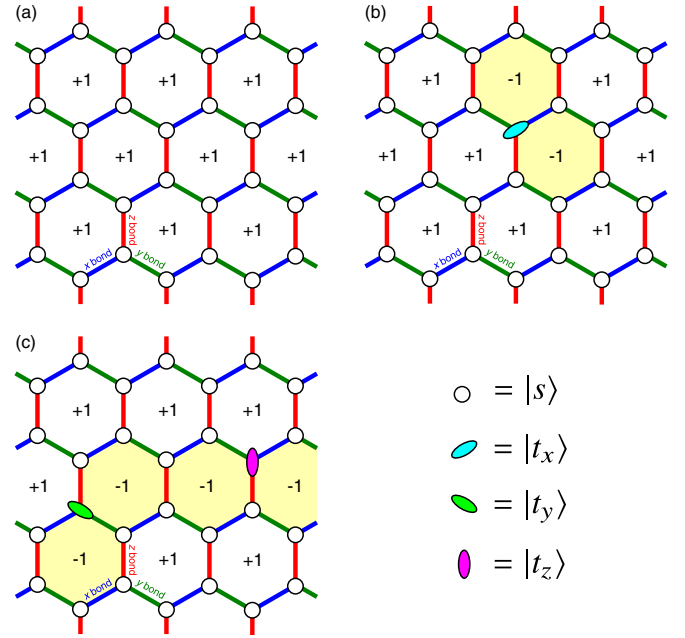


FIG. 2. Configurations of eigenvalues of X_p in (a) state $|\Phi_s\rangle$, where all dimers are spin singlets, (b) one-triplon state $|\Phi_{t_x}\rangle$, where an x component of the triplon is excited, and (c) two-triplon state $|\Phi_{t_y, t_z}\rangle$, where the y and z components of triplons are excited. Open circles represent spin singlets, and colored ellipses stand for the three different components of spin triplets, as shown in the legend. The shaded hexagons represent the plaquettes with $X_p = -1$.

$N = 24$ including 48 spins, where N is the number of dimers in the cluster. The clusters used in the present calculations are shown in Fig. 1(c). Note that the monolayer version of the $N = 24$ cluster has been widely used to obtain the phase diagram in the Kitaev-Heisenberg($-\Gamma$) models [51, 55, 59, 86]. In the ED calculations, we utilize the presence of the conserved quantities X_p and the parities P_s , P_{t_x} , P_{t_y} , and P_{t_z} to reduce the matrix dimensions. In addition to the ED calculations, we also make use of the bond-operator MF theory [77] and cluster expansion technique [78–80] to perform a comprehensive analysis. In the bond-operator MF theory, the local constraint is replaced by the global one by introducing the uniform chemical potential $\mu = \mu_i$, and the Bose condensation of singlets is assumed as $\langle s_i \rangle = \langle s_i^\dagger \rangle = \bar{s}$ [83–85]. Owing to these assumptions, the Hamiltonian is reduced to the free-boson system of the triplet excitations as

$$\begin{aligned}
 \mathcal{H}_{\text{MF}} = & \left(-\frac{3}{4} J_K \bar{s}^2 - \mu \bar{s}^2 + \mu \right) N + \left(\frac{J_H}{4} - \mu \right) \sum_{i, \alpha} t_{\alpha i}^\dagger t_{\alpha i} \\
 & - \frac{J_K \bar{s}^2}{2} \sum_{\langle ij \rangle_\alpha} (t_{\alpha i}^\dagger t_{\alpha j} + t_{\alpha i}^\dagger t_{\alpha j}^\dagger + \text{H.c.}), \quad (9)
 \end{aligned}$$

where we neglect the scattering terms between triplet excitations given in the second line of Eq. (6) and μ and \bar{s} are determined self-consistently.

We also use the cluster expansion technique [78–80], which is one of the powerful methods to discuss the quantum phase transitions in frustrated quantum spin systems such as J_1 – J_2 [87, 88], orthogonal-dimer [89–93], and Kitaev-Heisenberg

models [94,95]. In the bilayer model, we begin with interlayer dimer singlets [96,97]. As discussed before, parity symmetry for the number of singlets and triplets in our model exists, and therefore, odd-order coefficients never appear in the ground-state energy E_λ/N and spin correlations $\langle \mathbf{S}_{i,1} \cdot \mathbf{S}_{i,2} \rangle$. We compute the power series up to the 30th order for the above quantities. Furthermore, exploiting the first-order inhomogeneous differential method [98], we deduce the quantities far from the dimer limit $\lambda \rightarrow \infty$.

To examine thermodynamic quantities at finite temperatures, we employ the TPQ state approach [81,82]. In this paper, we treat the cluster with $N = 12$ [see Fig. 1(c)]. We prepare more than 20 random vectors for the initial states, and the physical quantities are calculated by averaging the values generated by these initial states.

IV. NUMERICAL RESULTS

A. Ground-state properties

In this section, we discuss ground-state properties of the bilayer Kitaev model given in Eq. (1). Figure 3(a) shows the ground-state energy $E_\lambda/(J_K + J_H)$ as a function of $\lambda/(1 + \lambda)$. We obtain the smooth curve using the ED calculations. We find that the energy obtained with the bond-operator MF approximation is lower than that of the ED. This should be due to its artifacts originating from the fact that triplet-triplet correlations are not taken into account correctly in the method. With increasing λ , the difference between the ED and bond-operator MF results becomes negligible, meaning that the bond-operator MF approximation is justified in the large- λ region. We also show the energy obtained with the cluster expansion method as the solid line in Fig. 3(a). Surprisingly, this almost coincides with the ED results except for $\lambda \lesssim 0.2$, although the method is also an approach from the large- λ limit. This indicates that the dimer-singlet state, which is adiabatically connected to the direct product state $|\Phi_s\rangle$, is realized in the region.

In the small- λ region, a large size dependence appears in the ED results, as shown in Fig. 3(b), in contrast to the large- λ region. With increasing system size, the energy in the limit of $\lambda = 0$ approaches the exact value, while it depends on the cluster shape. An important point is that the energy curve tends to have the bend structure around $\lambda \sim 0.06$.

The peculiar λ dependence of the ground-state energy can be clearly seen by taking its derivative. Figure 3(c) shows the second derivative of E_λ as a function of λ . It is found that the peak structure in each cluster develops with increasing system size while the dependence of the cluster shape is also observed. This indicates the existence of a first-order quantum phase transition at $\lambda = \lambda_c$ (~ 0.06) in the thermodynamic limit.

To clarify the nature of two distinct phases around λ_c , we also calculate the interlayer spin correlations $C_s = \frac{1}{N} \sum_i \langle \mathbf{S}_{i,1} \cdot \mathbf{S}_{i,2} \rangle$. The results are shown in Fig. 4(a) as a function of $\lambda/(1 + \lambda)$. When $\lambda \rightarrow \infty$, the spin singlet is realized in each dimer, and $C_s = -3/4$. In the large- λ region, the strong interlayer coupling stabilizes the dimer-singlet state with a short correlation length. Therefore, the ED results depend little on the cluster size and agree well with those obtained with

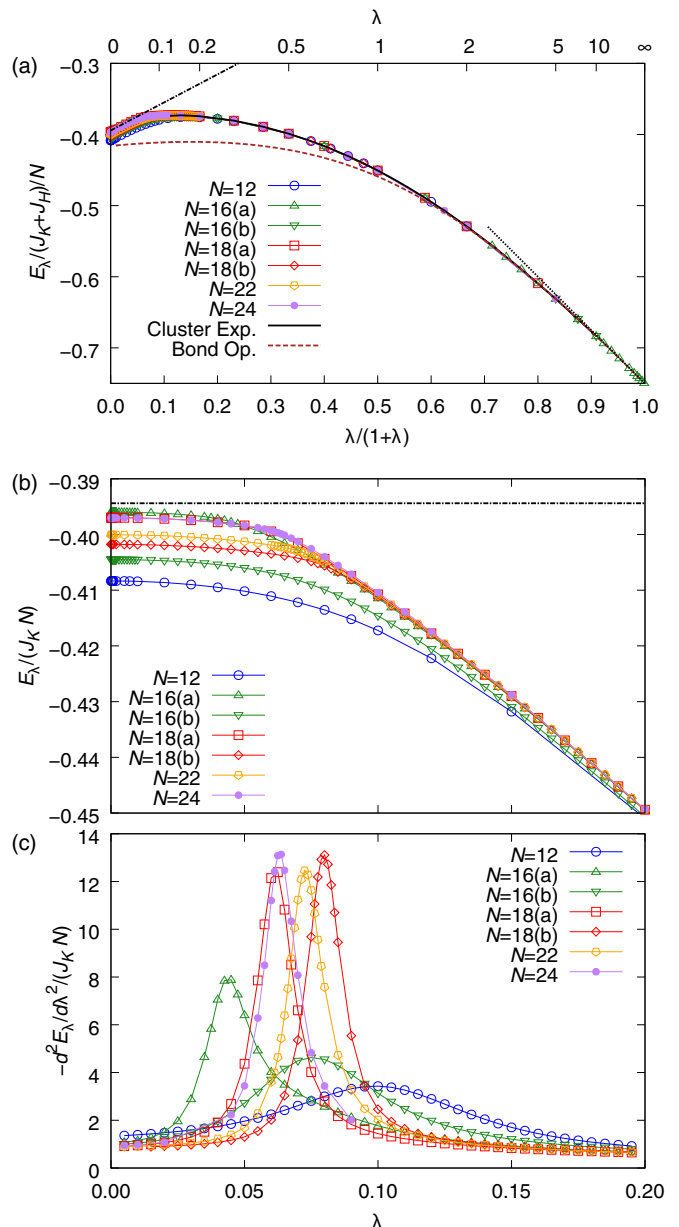


FIG. 3. (a) Ground-state energy $E_\lambda/(J_K + J_H)$ per dimer as a function of $\lambda/(1 + \lambda)$ in the bilayer Kitaev model. The upper axis shows the corresponding values of λ . The solid and dashed lines represent the results obtained with the cluster expansion and bond-operator MF theory. The symbols are obtained with the finite-size ED calculations. The dash-dotted and dotted lines represent the energies of the Kitaev QSL and dimer-singlet states, respectively. (b) Ground-state energy E_λ/J_K per dimer in the small- λ region. (c) Second derivative of the ground-state energy per dimer. Note that (b) and (c) are shown as a function of λ .

the cluster expansion, implying that the dimer-singlet state is realized in this region. With decreasing λ , the Ising coupling J_K suppresses interlayer spin correlations, and therefore, the absolute value of C_s decreases monotonically. Around $\lambda = \lambda_c$, a large cluster-size and shape dependence appears in the ED results, as shown in Fig. 4(b), and it is hard to extrapolate the quantity in the thermodynamic limit. Nevertheless, the

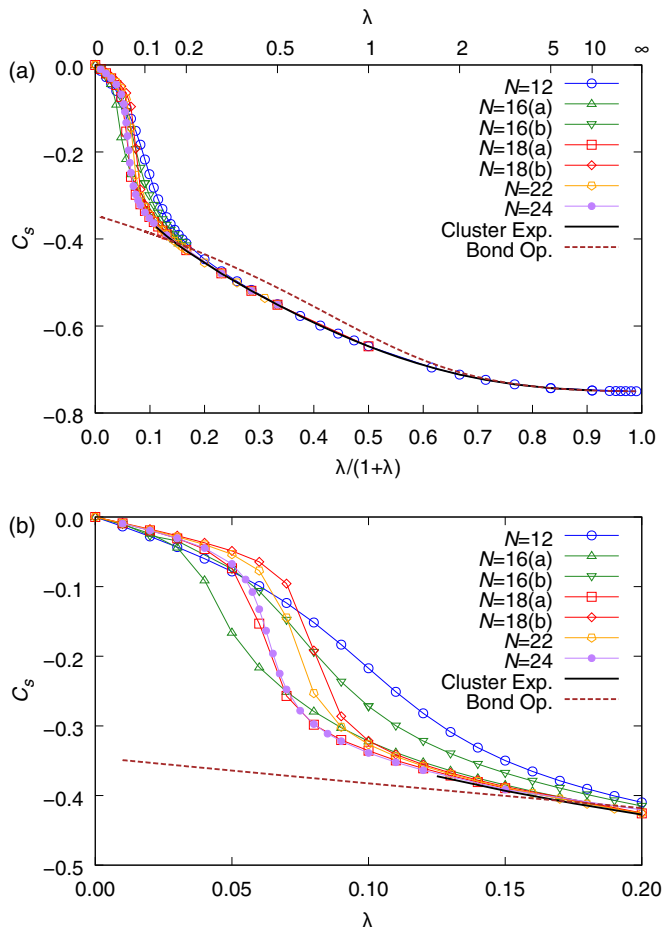


FIG. 4. (a) Interlayer dimer spin correlation C_s as a function of $\lambda/(1+\lambda)$ and (b) the magnified plot of C_s as a function of λ in the small- λ region. The solid and dashed lines represent the results obtained by the cluster expansion and bond operator MF theory, and the symbols are obtained with the finite-size ED calculations.

results for the larger clusters are still consistent with the cluster expansion, which implies that the dimer-singlet state is realized when $\lambda > \lambda_c$.

On the other hand, in the smaller- λ region, the spin correlation suddenly changes and takes a smaller value, suggesting the realization of the Kitaev QSL expected in the two independent Kitaev models. To reinforce the above discussion, we calculate the expectation value of the local Z_2 conserved quantity of the monolayer Kitaev model $\langle W_p \rangle$. This takes +1 for all plaquettes in the Kitaev QSL ground state realized at $\lambda = 0$, whereas it is expected to vanish in the dimer-singlet state. Therefore, $\langle W_p \rangle$ is an appropriate quantity to characterize the Kitaev QSL. The λ dependence of $\langle W_p \rangle$ for the $N = 24$ cluster is shown in Fig. 5. It is found that $\langle W_p \rangle$ rapidly decreases from +1 around $\lambda \sim 0.06$, where its derivative has a sharp peak. The results indicate that the Kitaev QSL is realized in $\lambda \lesssim 0.06$. Furthermore, the coincidence of the values of λ , at which $\langle W_p \rangle$ and the interlayer dimer correlation C_s exhibit abrupt changes, suggests the existence of the first-order phase transition between the Kitaev QSL and interlayer dimer-singlet states at $\lambda = \lambda_c \sim 0.06$. It is worth noting that $\lambda_c = J_{Hc}/J_K \sim 0.06$ is close to the spin gap of the pure Kitaev model, $\Delta_K/J_K \sim 0.065$. This implies

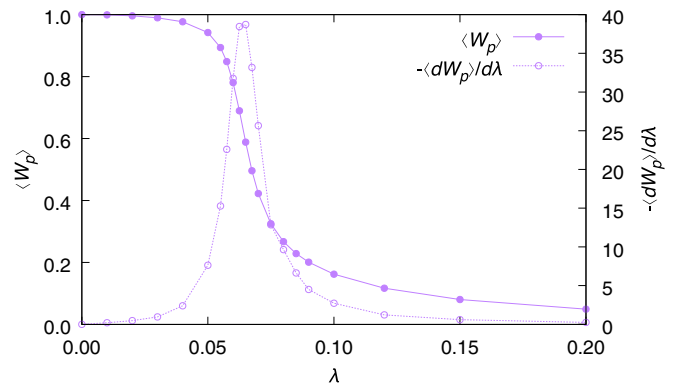


FIG. 5. Expectation value of the local conserved quantity of the monolayer Kitaev model W_p and its first derivative as a function of λ , which are obtained with the ED on the $N = 24$ cluster.

that the Kitaev QSL against the interlayer Heisenberg coupling is maintained by the existence of the spin gap inherent in the Kitaev model.

B. Excitation spectrum

Next, we discuss the excitation structure of the bilayer Kitaev model. It is known that in the Kitaev model ($\lambda = 0$), there is a Majorana continuum in the excited states. On the other hand, in the dimer limit $\lambda \rightarrow \infty$, due to the spin gap with the excitation energy J_H , discrete excited levels appear, corresponding to the number of triplons. Here, we first analyze the excitation spectrum by means of the bond operator method. The MF Hamiltonian (9) indicates that the α component of the local triplet excitation is hybridized only with that on the same α bond. Thus, the triplet excitation t_α is localized on each α bond and forms the bonding and antibonding states. Figure 6

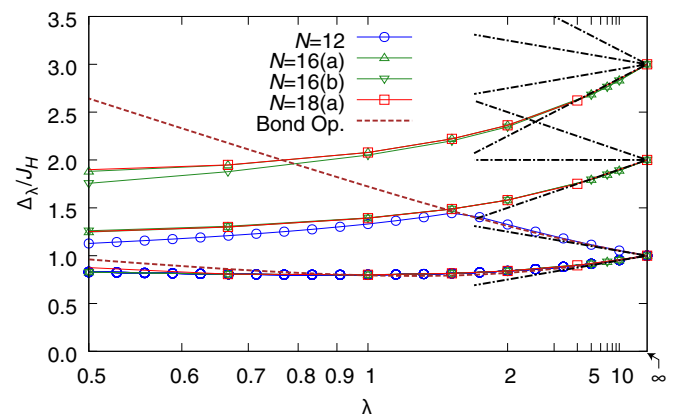


FIG. 6. The λ dependence of the excitation energy Δ_λ . The symbols and dashed lines represent the results obtained with the ED method and bond-operator MF theory, respectively. For the $N = 12$ cluster, excitation energies up to 19th excited state are presented. For the other clusters, excitation energies are calculated from the lowest-energy states of the following subspaces: $(P_x, P_y, P_z) = (-1, +1, +1), (-1, -1, +1),$ and $(-1, -1, -1)$. The dash-dotted lines represent the excitation energies expected from the localized bonding and antibonding energy levels, $1 \pm 1/(2\lambda), 2 \pm 1/\lambda, 2, 3 \pm 1/(2\lambda), 3 \pm 3/(2\lambda)$, in the large- λ limit.

shows the one-body spectrum of the triplet excitation obtained with the bond-operator MF approximation. The introduction of the Kitaev interaction splits the excitation energy of the spin gap into two levels, which corresponds to the formation of the bonding and antibonding states.

The fact that triplet excitations are localized on the corresponding NN bonds can be confirmed exactly by considering the spatial configuration of the local conserved quantity X_p . This is done in a manner similar to the proof for the absence of the long-range spin correlations in the monolayer Kitaev model [8]. As shown in Fig. 2(b), in the one-triplon state $|\Phi_{t_x,i}\rangle$ on dimer site i , the two eigenvalues of X_p are flipped from the ground state. On the other hand, the one-triplon state $|\Phi_{t_x,j}\rangle$ on another dimer site j possesses a different configuration of eigenvalues of X_p , and therefore, $\langle \Phi_{t_x,i} | \Phi_{t_x,j} \rangle = \langle \Phi_s | \tilde{t}_{x,i}^\dagger \tilde{t}_{x,j}^\dagger | \Phi_s \rangle = 0$ is expected for the case where i and j are on the same x bond. As for one-triplon state with a different component, $|\Phi_{t_\alpha,j}\rangle$ ($\alpha \neq x$), its parity is different from that of state $|\Phi_{t_x,j}\rangle$, and these two states are never hybridized. From the above consideration, localized bonding and antibonding states for the one-triplon excitation are each $(3N/2)$ -fold degenerate. The corresponding energies are $\Delta_{\pm}/J_H = 1 \pm 1/(2\lambda) + 3/(8\lambda^2) + \dots$. In addition, one can consider multi-triplon excitations, which are shown as the dash-dotted lines in Fig. 6. Note that a pair of triplons with the α component on an α bond can be mixed with the singlet state $|\Phi_s\rangle$, and hence, the bound state may have a dispersion in the presence of the Kitaev interaction with $O(1/\lambda^2)$. Furthermore, two triplon states with different components should form the bound state. Therefore, two triplon states should be split into some dispersionless bound states and dispersive bands on the introduction of the Kitaev coupling J_K .

To confirm the above consideration, we calculate the excitation spectrum using the ED method. The results are presented in Fig. 6. The low-energy spectra obtained by the bond-operator MF approximation are well reproduced by the finite-size calculation in the large- λ case because of the existence of the localized excitations. We have also confirmed that the first and second excited states in $\lambda \gtrsim 1.5$ are $(3N/2)$ -fold degenerate, which is adiabatically connected to $3N$ -fold degenerate states coming from local triplet excitations at $\lambda \rightarrow \infty$. These degeneracies are consistent with those of the bonding and antibonding states of the triplet excitations discussed above. At $\lambda \sim 1.5$, excitation energies originating from one-triplon and two-triplon excited states intersect without mixing. This is understood from the fact that the parity of the triplon number is conserved in the present system, which prohibits mixing between one-triplon and two-triplon excited states. We wish to note that the lowest excitation energy is always finite in the case with $\lambda \gtrsim 0.06$. Furthermore, we cannot find any tendency for closing the gap. This is consistent with the fact that the dimer-singlet state is realized in the region $\lambda > \lambda_c$.

In the Kitaev limit, the excitation spectrum shows a continuum coming from the Majorana fermions, as mentioned before. On the other hand, low-energy one-triplon states are localized, and their excitation energy may be proportional to the interlayer spin correlation C_s . We expect that, with decreasing λ , the discrete levels will disappear at the first-order quantum phase transition point λ_c and the Majorana continuum

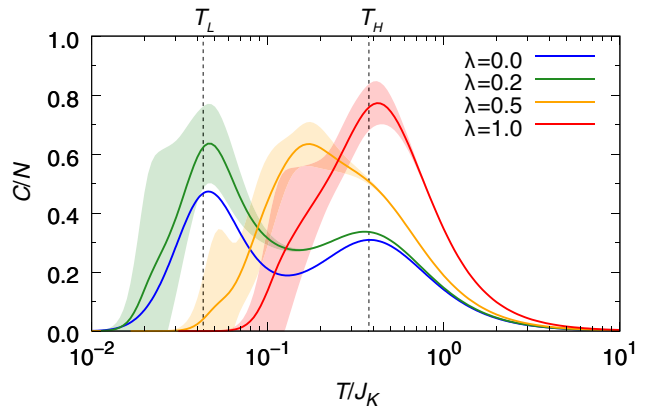


FIG. 7. The specific heat per dimer C/N as a function of the temperature for the $N = 12$ cluster when $\lambda = 0, 0.1, 0.5$, and 1 . Shaded areas are the possible errors estimated by using the standard deviation of the results obtained from more than 20 initial random states in the TPQ calculations, and the result for $\lambda = 0$ is obtained with the full diagonalization. The dashed lines represent the peak temperatures denoted by T_L and T_H at $\lambda = 0$.

might appear below λ_c . However, larger cluster calculations are needed to clarify the spectral change around λ_c , and this remains for a future work.

V. FINITE-TEMPERATURE PROPERTIES

Finally, we discuss the finite-temperature properties of the bilayer Kitaev model. Figure 7 shows the temperature dependence of the specific heat for several values of λ by using the TPQ state approach for the $N = 12$ cluster. When $\lambda = 0$, the system is reduced to the decoupled Kitaev models, and the double-peak structure appears at $T = T_L \sim 0.044J_K$ and $T_H \sim 0.38J_K$ in the $N = 12$ cluster. This is consistent with the fact that the spin degrees of freedom are split into itinerant Majorana fermions and localized gauge fluxes in each monolayer Kitaev model. In comparison with the curves with $\lambda = 0.2$, the lower characteristic temperature T_L slightly shifts

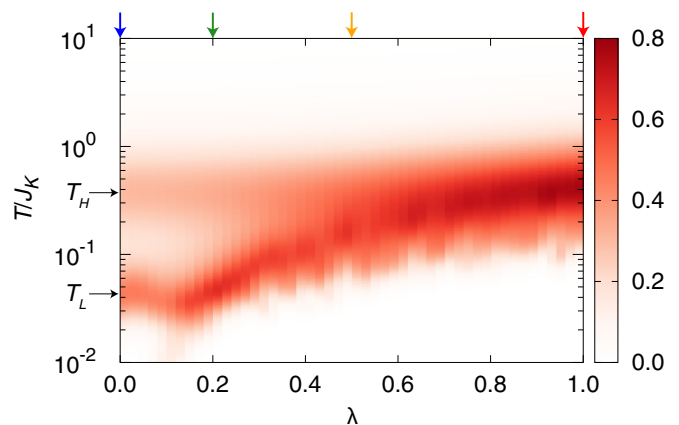


FIG. 8. Density plot of the specific heat in the T - λ plane obtained with the TPQ method on the $L = 12$ cluster. The arrows represent the corresponding temperatures used in Fig. 7. T_L and T_H stand for the peak temperatures of the specific heat at $\lambda = 0$.

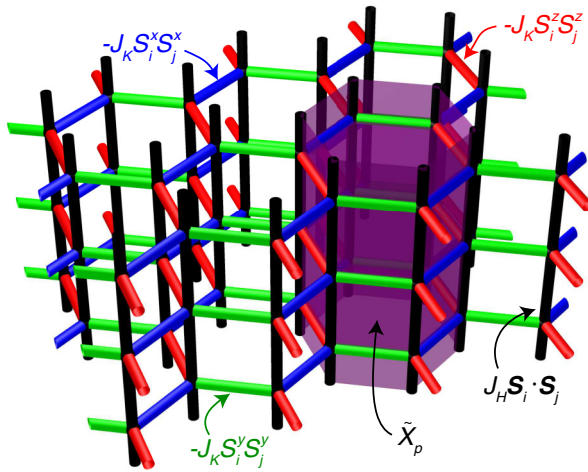


FIG. 9. Schematic picture of the multilayer Kitaev model with interlayer Heisenberg couplings. The local conserved quantity \tilde{X}_p is depicted.

to higher temperatures, while the other little shifts. With further increasing λ , these two peaks merge into a single peak, which is a Schottky-type peak characteristic of the gapped systems.

To clarify how the double-peak structure of the monolayer Kitaev model is gradually changed by the introduction of the interlayer coupling, we show in Fig. 8 the density plot of the specific heat on the plane of λ and temperature. The double peaks appearing at $\lambda = 0$ are clearly seen below $\lambda \sim 0.2$. With increasing λ , the temperature of the higher-temperature peak hardly changes, whereas the lower one depends on λ . We find that these peaks merge into the single peak around $\lambda \sim 0.6$. This suggests that the proximity effect of the Kitaev QSL emerges at higher temperatures even above λ_c . A similar effect has been discussed in the Kitaev-Heisenberg model, where the double-peak structure is seen even in the magnetic ordered phase close to the Kitaev QSL ground state [64].

VI. DISCUSSION

In this section, we briefly discuss the magnetic properties of multilayer Kitaev systems, where the Kitaev layers are connected by the Heisenberg couplings, as shown in Fig. 9. In the system, we can define the local Z_2 conserved quantity $\tilde{X}_p = \prod_n W_{p,n}$ (see Fig. 9) by straightforward generalization of W_p defined in the bilayer system, as discussed in the previous sections. When the number of layers is large enough,

this system is regarded as one-dimensional Heisenberg chains coupled with Kitaev interactions. In this case, its spin correlation length shows power-law decay along each chain direction. However, the existence of the local conserved quantity \tilde{X}_p indicates that there are no spin correlations except for NN sites in each Kitaev layer and sites belonging to the same Heisenberg chain. This suggests that the ground state of the stacked Kitaev model with the interlayer Heisenberg couplings shown Fig. 9 is nonmagnetic as three-dimensional longer-range spin correlations are absent. However, there is a possibility that quantum phase transitions between nonmagnetic phases take place as in the bilayer system. This is an interesting issue but is beyond the scope of the present study.

VII. SUMMARY

In summary, we have investigated the ground-state and finite-temperature properties of the bilayer Kitaev model. The results obtained with the ED, bond-operator MF, and cluster expansion methods suggest the existence of a first-order quantum phase transition between the Kitaev QSL and dimer-singlet states in the thermodynamic limit. In the excitation spectrum, an excited single triplon is localized in the dimer-singlet phase, which is proved by the existence of a local conserved quantity. We have also discussed the finite-temperature properties, where the double-peak structure intrinsic to the Kitaev QSL appears even in the dimer-singlet phase near the phase boundary. Furthermore, we have shown that three-dimensional long-range spin correlations are also absent in the stacked multilayer Kitaev systems with arbitrary layer numbers. The present results will stimulate studies for possible extensions of the layered Kitaev model by introducing, for example, the magnetic field and the in-plane Heisenberg and/or Γ terms. Moreover, the results might provide insight into recent experimental studies on thin films of iridium and ruthenium compounds [73–76].

ACKNOWLEDGMENTS

The authors would like to thank S. Suga for valuable discussions. This work is supported by a Grant-in-Aid for Scientific Research from JSPS and KAKENHI Grants No. JP17K05536 and No. JP16H01066 (A.K.) and No. JP16K17747, No. JP16H02206, and No. JP16H00987 (J.N.). Parts of the numerical calculations were performed on the supercomputing systems in ISSP, the University of Tokyo.

- [1] P. W. Anderson, *Mater. Res. Bull.* **8**, 153 (1973).
- [2] L. Balents, *Nature (London)* **464**, 199 (2010).
- [3] Y. Zhou, K. Kanoda, and T.-K. Ng, *Rev. Mod. Phys.* **89**, 025003 (2017).
- [4] L. Savary and L. Balents, *Rep. Prog. Phys.* **80**, 016502 (2017).
- [5] A. Kitaev, *Ann. Phys. (NY)* **321**, 2 (2006).
- [6] S. Trebst, [arXiv:1701.07056](https://arxiv.org/abs/1701.07056).
- [7] M. Hermanns, I. Kimchi, and J. Knolle, [arXiv:1705.01740](https://arxiv.org/abs/1705.01740).
- [8] G. Baskaran, S. Mandal, and R. Shankar, *Phys. Rev. Lett.* **98**, 247201 (2007).

- [9] J. Knolle, D. L. Kovrizhin, J. T. Chalker, and R. Moessner, *Phys. Rev. Lett.* **112**, 207203 (2014).
- [10] X.-Y. Feng, G.-M. Zhang, and T. Xiang, *Phys. Rev. Lett.* **98**, 087204 (2007).
- [11] H.-D. Chen and J. Hu, *Phys. Rev. B* **76**, 193101 (2007).
- [12] H.-D. Chen and Z. Nussinov, *J. Phys. A* **41**, 075001 (2008).
- [13] F. L. Pedrocchi, S. Chesi, and D. Loss, *Phys. Rev. B* **84**, 165414 (2011).
- [14] J. Nasu, M. Udagawa, and Y. Motome, *Phys. Rev. Lett.* **113**, 197205 (2014).

- [15] J. Nasu, M. Udagawa, and Y. Motome, *Phys. Rev. B* **92**, 115122 (2015).
- [16] G. Jackeli and G. Khaliullin, *Phys. Rev. Lett.* **102**, 017205 (2009).
- [17] Y. Singh and P. Gegenwart, *Phys. Rev. B* **82**, 064412 (2010).
- [18] Y. Singh, S. Manni, J. Reuther, T. Berlijn, R. Thomale, W. Ku, S. Trebst, and P. Gegenwart, *Phys. Rev. Lett.* **108**, 127203 (2012).
- [19] R. Comin, G. Levy, B. Ludbrook, Z.-H. Zhu, C. N. Veenstra, J. A. Rosen, Y. Singh, P. Gegenwart, D. Stricker, J. N. Hancock, D. van der Marel, I. S. Elfimov, and A. Damascelli, *Phys. Rev. Lett.* **109**, 266406 (2012).
- [20] S. K. Choi, R. Coldea, A. N. Kolmogorov, T. Lancaster, I. I. Mazin, S. J. Blundell, P. G. Radaelli, Y. Singh, P. Gegenwart, K. R. Choi, S.-W. Cheong, P. J. Baker, C. Stock, and J. Taylor, *Phys. Rev. Lett.* **108**, 127204 (2012).
- [21] K. W. Plumb, J. P. Clancy, L. J. Sandilands, V. V. Shankar, Y. F. Hu, K. S. Burch, H.-Y. Kee, and Y.-J. Kim, *Phys. Rev. B* **90**, 041112 (2014).
- [22] Y. Kubota, H. Tanaka, T. Ono, Y. Narumi, and K. Kindo, *Phys. Rev. B* **91**, 094422 (2015).
- [23] J. A. Sears, M. Songvilay, K. W. Plumb, J. P. Clancy, Y. Qiu, Y. Zhao, D. Parshall, and Y.-J. Kim, *Phys. Rev. B* **91**, 144420 (2015).
- [24] M. Majumder, M. Schmidt, H. Rosner, A. A. Tsirlin, H. Yasuoka, and M. Baenitz, *Phys. Rev. B* **91**, 180401 (2015).
- [25] S. Bette, T. Takayama, K. Kitagawa, R. Takano, H. Takagi, and R. E. Dinnebier, *Dalton Trans.* **46**, 15216 (2017).
- [26] L. J. Sandilands, Y. Tian, K. W. Plumb, Y.-J. Kim, and K. S. Burch, *Phys. Rev. Lett.* **114**, 147201 (2015).
- [27] A. Banerjee, C. Bridges, J.-Q. Yan, A. Aczel, L. Li, M. Stone, G. Granroth, M. Lumsden, Y. Yiu, J. Knolle *et al.*, *Nat. Mater.* **15**, 733 (2016).
- [28] A. Banerjee, J. Yan, J. Knolle, C. A. Bridges, M. B. Stone, M. D. Lumsden, D. G. Mandrus, D. A. Tennant, R. Moessner, and S. E. Nagler, *Science* **356**, 1055 (2017).
- [29] S.-H. Do, S.-Y. Park, J. Yoshitake, J. Nasu, Y. Motome, Y. S. Kwon, D. Adroja, D. Voneshen, K. Kim, T.-H. Jang, J.-H. Park, K.-Y. Choi, and S. Ji, *Nat. Phys.* **13**, 1079 (2017).
- [30] D. Hirobe, M. Sato, Y. Shiomi, H. Tanaka, and E. Saitoh, *Phys. Rev. B* **95**, 241112 (2017).
- [31] I. A. Leahy, C. A. Pocs, P. E. Siegfried, D. Graf, S.-H. Do, K.-Y. Choi, B. Normand, and M. Lee, *Phys. Rev. Lett.* **118**, 187203 (2017).
- [32] R. Hentrich, A. U. B. Wolter, X. Zotos, W. Brenig, D. Nowak, A. Isaeva, T. Doert, A. Banerjee, P. Lampen-Kelley, D. G. Mandrus, S. E. Nagler, J. Sears, Y.-J. Kim, B. Büchner, and C. Hess, *arXiv:1703.08623*.
- [33] Y. Kasahara, K. Sugii, T. Ohnishi, M. Shimozawa, M. Yamashita, N. Kurita, H. Tanaka, J. Nasu, Y. Motome, T. Shibauchi, and Y. Matsuda, *arXiv:1709.10286*.
- [34] I. I. Mazin, H. O. Jeschke, K. Foyevtsova, R. Valentí, and D. I. Khomskii, *Phys. Rev. Lett.* **109**, 197201 (2012).
- [35] J. Knolle, G.-W. Chern, D. L. Kovrizhin, R. Moessner, and N. B. Perkins, *Phys. Rev. Lett.* **113**, 187201 (2014).
- [36] F. Zschocke and M. Vojta, *Phys. Rev. B* **92**, 014403 (2015).
- [37] H.-S. Kim, V. Shankar V., A. Catuneanu, and H.-Y. Kee, *Phys. Rev. B* **91**, 241110(R) (2015).
- [38] M. Vojta, A. K. Mitchell, and F. Zschocke, *Phys. Rev. Lett.* **117**, 037202 (2016).
- [39] J. Nasu, J. Knolle, D. L. Kovrizhin, Y. Motome, and R. Moessner, *Nat. Phys.* **12**, 912 (2016).
- [40] S. Rachel, L. Fritz, and M. Vojta, *Phys. Rev. Lett.* **116**, 167201 (2016).
- [41] J. Yoshitake, J. Nasu, and Y. Motome, *Phys. Rev. Lett.* **117**, 157203 (2016).
- [42] J. Yoshitake, J. Nasu, Y. Kato, and Y. Motome, *Phys. Rev. B* **96**, 024438 (2017).
- [43] J. Yoshitake, J. Nasu, and Y. Motome, *Phys. Rev. B* **96**, 064433 (2017).
- [44] J. Nasu, J. Yoshitake, and Y. Motome, *Phys. Rev. Lett.* **119**, 127204 (2017).
- [45] A. Metavitsiadis, A. Pidotella, and W. Brenig, *Phys. Rev. B* **96**, 205121 (2017).
- [46] A. M. Samarakoon, A. Banerjee, S.-S. Zhang, Y. Kamiya, S. E. Nagler, D. A. Tennant, S.-H. Lee, and C. D. Batista, *Phys. Rev. B* **96**, 134408 (2017).
- [47] P. Fendley, *J. Stat. Mech.* (2012) P11020.
- [48] A. Vaezi, *Phys. Rev. B* **90**, 075106 (2014).
- [49] M. Barkeshli, H.-C. Jiang, R. Thomale, and X.-L. Qi, *Phys. Rev. Lett.* **114**, 026401 (2015).
- [50] F. Ye, S. Chi, H. Cao, B. C. Chakoumakos, J. A. Fernandez-Baca, R. Custelcean, T. F. Qi, O. B. Korneta, and G. Cao, *Phys. Rev. B* **85**, 180403(R) (2012).
- [51] J. Chaloupka, G. Jackeli, and G. Khaliullin, *Phys. Rev. Lett.* **105**, 027204 (2010).
- [52] H.-C. Jiang, Z.-C. Gu, X.-L. Qi, and S. Trebst, *Phys. Rev. B* **83**, 245104 (2011).
- [53] I. Kimchi and Y.-Z. You, *Phys. Rev. B* **84**, 180407 (2011).
- [54] J. Reuther, R. Thomale, and S. Trebst, *Phys. Rev. B* **84**, 100406 (2011).
- [55] J. Chaloupka, G. Jackeli, and G. Khaliullin, *Phys. Rev. Lett.* **110**, 097204 (2013).
- [56] K. Foyevtsova, H. O. Jeschke, I. I. Mazin, D. I. Khomskii, and R. Valentí, *Phys. Rev. B* **88**, 035107 (2013).
- [57] V. M. Katukuri, S. Nishimoto, V. Yushankhai, A. Stoyanova, H. Kandpal, S. Choi, R. Coldea, I. Rousochatzakis, L. Hozoi, and J. van den Brink, *New J. Phys.* **16**, 013056 (2014).
- [58] Y. Yamaji, Y. Nomura, M. Kurita, R. Arita, and M. Imada, *Phys. Rev. Lett.* **113**, 107201 (2014).
- [59] J. G. Rau, E. K.-H. Lee, and H.-Y. Kee, *Phys. Rev. Lett.* **112**, 077204 (2014).
- [60] J. Nasu and Y. Motome, *Phys. Rev. B* **90**, 045102 (2014).
- [61] K. Shinjo, S. Sota, and T. Tohyama, *Phys. Rev. B* **91**, 054401 (2015).
- [62] T. Suzuki, T. Yamada, Y. Yamaji, and S.-I. Suga, *Phys. Rev. B* **92**, 184411 (2015).
- [63] J. Chaloupka and G. Khaliullin, *Phys. Rev. B* **94**, 064435 (2016).
- [64] Y. Yamaji, T. Suzuki, T. Yamada, S.-I. Suga, N. Kawashima, and M. Imada, *Phys. Rev. B* **93**, 174425 (2016).
- [65] Y. Sizyuk, P. Wölfle, and N. B. Perkins, *Phys. Rev. B* **94**, 085109 (2016).
- [66] X.-Y. Song, Y.-Z. You, and L. Balents, *Phys. Rev. Lett.* **117**, 037209 (2016).
- [67] T. Okubo, K. Shinjo, Y. Yamaji, N. Kawashima, S. Sota, T. Tohyama, and M. Imada, *Phys. Rev. B* **96**, 054434 (2017).
- [68] S. M. Winter, K. Riedl, P. A. Maksimov, A. L. Chernyshev, A. Honecker, and R. Valentí, *Nat. Commun.* **8**, 1152 (2017).
- [69] A. Catuneanu, Y. Yamaji, G. Wachtel, H.-Y. Kee, and Y. B. Kim, *arXiv:1701.07837*.

- [70] A. Koga, S. Nakauchi, and J. Nasu, [arXiv:1705.09659](https://arxiv.org/abs/1705.09659).
- [71] H. B. Cao, A. Banerjee, J.-Q. Yan, C. A. Bridges, M. D. Lumsden, D. G. Mandrus, D. A. Tennant, B. C. Chakoumakos, and S. E. Nagler, *Phys. Rev. B* **93**, 134423 (2016).
- [72] K. Slagle, W. Choi, L. E. Chern, and Y. B. Kim, [arXiv:1710.01307](https://arxiv.org/abs/1710.01307).
- [73] M. Ziatdinov, A. Banerjee, A. Maksov, T. Berlijn, W. Zhou, H. Cao, J.-Q. Yan, C. A. Bridges, D. Mandrus, S. E. Nagler *et al.*, *Nat. Commun.* **7**, 13774 (2016).
- [74] D. Weber, L. M. Schoop, V. Duppel, J. M. Lippmann, J. Nuss, and B. V. Lotsch, *Nano Lett.* **16**, 3578 (2016).
- [75] M. Jenderka, J. Barzola-Quiquia, Z. Zhang, H. Frenzel, M. Grundmann, and M. Lorenz, *Phys. Rev. B* **88**, 045111 (2013).
- [76] M. Jenderka, R. Schmidt-Grund, M. Grundmann, and M. Lorenz, *J. Appl. Phys.* **117**, 025304 (2015).
- [77] S. Sachdev and R. N. Bhatt, *Phys. Rev. B* **41**, 9323 (1990).
- [78] R. R. P. Singh, M. P. Gelfand, and D. A. Huse, *Phys. Rev. Lett.* **61**, 2484 (1988).
- [79] M. Gelfand, R. Singh, and D. A. Huse, *J. Stat. Phys.* **59**, 1093 (1996).
- [80] M. Gelfand, *Solid State Commun.* **98**, 11 (1996).
- [81] S. Sugiura and A. Shimizu, *Phys. Rev. Lett.* **108**, 240401 (2012).
- [82] S. Sugiura and A. Shimizu, *Phys. Rev. Lett.* **111**, 010401 (2013).
- [83] S. Gopalan, T. M. Rice, and M. Sigrist, *Phys. Rev. B* **49**, 8901 (1994).
- [84] V. N. Kotov, O. Sushkov, Z. Weihong, and J. Oitmaa, *Phys. Rev. Lett.* **80**, 5790 (1998).
- [85] Y. Matsushita, M. P. Gelfand, and C. Ishii, *J. Phys. Soc. Jpn.* **68**, 247 (1999).
- [86] S. Okamoto, *Phys. Rev. B* **87**, 064508 (2013).
- [87] M. P. Gelfand, R. R. P. Singh, and D. A. Huse, *Phys. Rev. B* **40**, 10801 (1989).
- [88] O. P. Sushkov, J. Oitmaa, and Z. Weihong, *Phys. Rev. B* **63**, 104420 (2001).
- [89] Z. Weihong, C. J. Hamer, and J. Oitmaa, *Phys. Rev. B* **60**, 6608 (1999).
- [90] A. Koga and N. Kawakami, *Phys. Rev. Lett.* **84**, 4461 (2000).
- [91] A. Koga, *J. Phys. Soc. Jpn.* **69**, 3509 (2000).
- [92] C. Knetter, A. Bühler, E. Müller-Hartmann, and G. S. Uhrig, *Phys. Rev. Lett.* **85**, 3958 (2000).
- [93] Y. Takushima, A. Koga, and N. Kawakami, *J. Phys. Soc. Jpn.* **70**, 1369 (2001).
- [94] J. Oitmaa, *Phys. Rev. B* **92**, 020405 (2015).
- [95] R. R. P. Singh and J. Oitmaa, *Phys. Rev. B* **96**, 144414 (2017).
- [96] K. Hida, *J. Phys. Soc. Jpn.* **67**, 1540 (1998).
- [97] K. Hida, *J. Phys. Soc. Jpn.* **61**, 1013 (1992).
- [98] A. J. Guttmann, in *Phase Transitions and Critical Phenomena*, edited by C. Domb and J. L. Lebowitz (Academic Press, New York, 1989), Vol. 13, p. 1.